Eur. J. Biochem. **271**, 792–800 (2004) © FEBS 2004 doi:10.1111/j.1432-1033.2004.03983.x

FRET evidence for a conformational change in TFIIB upon TBP-DNA binding

Le Zheng[1], Klaus P. Hoeflich[1], Laura M. Elsby[2], Mahua Ghosh[1], Stefan G. E. Roberts[2] and Mitsuhiko Ikura[1]

[1]*Division of Molecular and Structural Biology, Ontario Cancer Institute and Department of Medical Biophysics, University of Toronto, Ontario, Canada;* [2]*Division of Gene Regulation and Bioinformatics, School of Biological Sciences, University of Manchester, UK*

As a critical step of the preinitiation complex assembly in transcription, the general transcription factor TFIIB forms a complex with the TATA-box binding protein (TBP) bound to a promoter element. Transcriptional activators such as the herpes simplex virus VP16 facilitate this complex formation through conformational activation of TFIIB, a focal molecule of transcriptional initiation and activation. Here, we used fluorescence resonance energy transfer to investigate conformational states of human TFIIB fused to enhanced cyan fluorescent protein and enhanced yellow fluorescent protein at its N- and C-terminus, respectively. A significant reduction in fluorescence resonance energy transfer ratio was observed when this fusion protein, hereafter named CYIIB, was mixed with promoter-loaded TBP. The rate for the TFIIB–TBP–DNA complex formation is accelerated drastically by GAL4-VP16 and is also dependent on the type of promoter sequences. These results provide compelling evidence for a 'closed-to-open' conformational change of TFIIB upon binding to the TBP–DNA complex, which probably involves alternation of the spatial orientation between the N-terminal zinc ribbon domain and the C-terminal conserved core domain responsible for direct interactions with TBP and a DNA element.

Keywords: TFIIB; TATA-box binding protein; VP16; fluorescence resonance energy transfer; adenovirus major late promoter.

The general transcription factor TFIIB plays a crucial role in the assembly of the transcriptional preinitiation complex (PIC) by recognizing the TATA binding protein (TBP) bound to the TATA element and by recruiting RNA polymerase II (Pol II) and TFIIF into the PIC [1–3]. Consistent with the central function of TFIIB in the initial step of the PIC formation, TFIIB has been proposed to be a target of transcriptional activators [4–6]. Human TFIIB, consisting of 316 amino acid residues, is comprised of a N-terminal domain (NTD) that contains the Zn^{2+} ribbon motif, and a C-terminal core domain (CTD) possessing two repeats of the cyclin fold [7] (Fig. 1A). The two functionally distinct domains are connected via a highly conserved linker containing several charged residues, hereafter termed a charged cluster domain (CCD), critical for maintaining TFIIB conformation [5,8,9].

In 1994, Roberts and Green [4] proposed a mechanism for the activator-dependent transcriptional activation that involves a closed-to-open conformational change in TFIIB. In isolation, or presumably in the holoenzyme-bound state, TFIIB bears a strong interaction between the NTD and CTD, thus forming a compact structure as a whole. Upon binding to a TBP-promoter complex, this intramolecular interaction may be weakened by an ill-defined mechanism such that the TFIIB CTD can then interact with the core domain of TBP (TBPc) and the core promoter element and the TFIIB NTD can recruit Pol II and TFIIF into the initiation site. Transcriptional activators such as VP16 are believed to facilitate this conformational change in TFIIB, thereby promoting accelerated formation of the PIC and an increase in mRNA synthesis. More recently, biochemical studies [9,10] have shown that TFIIB can make sequence-specific DNA contact with an element immediately upstream of the TATA box, called the TFIIB recognition element (BRE). Proposed functions of this TFIIB–BRE interaction include modulation of the strength of the core promoter and the proper positioning of the TFIIB–TBP–TATA complex with respect to the initiation site influencing the start site selection. These studies suggest essential roles of the orientation of NTD–CTD in TFIIB conformational activation in expression of its biological functions.

In order to probe the TFIIB conformational change and to investigate the static and kinetic properties of the TFIIB–TBP-promoter complex formation, we used fluorescence

Correspondence to M. Ikura, Division of Molecular and Structural Biology, Ontario Cancer Institute and Department of Medical Biophysics, University of Toronto, 610 University Avenue, Ontario, M5G 2M9, Canada. Fax: + 01 416 946 2055, E-mail: mikura@uhnres.utoronto.ca

Abbreviations: AdE4, adenovirus E4 promoter; AdML, adenovirus major late promoter; BRE, TFIIB recognition element; CCD, charged cluster domain; CTD, C-terminal domain; CYIIB, TFIIB fused with ECFP and EYFP at the N- and C-terminus; ECFP, enhanced cyan fluorescent protein; EYFP, enhanced yellow fluorescent protein; FRET, fluorescence resonance energy transfer; TBP, TATA-box binding protein; NTD, N-terminal domain; PIC, preinitiation complex; pol II, RNA polymerase II; TBPc, the core domain of TBP; TFIIBc, the core domain of TFIIB.

(Received 16 October 2003, revised 5 December 2003, accepted 7 January 2004)

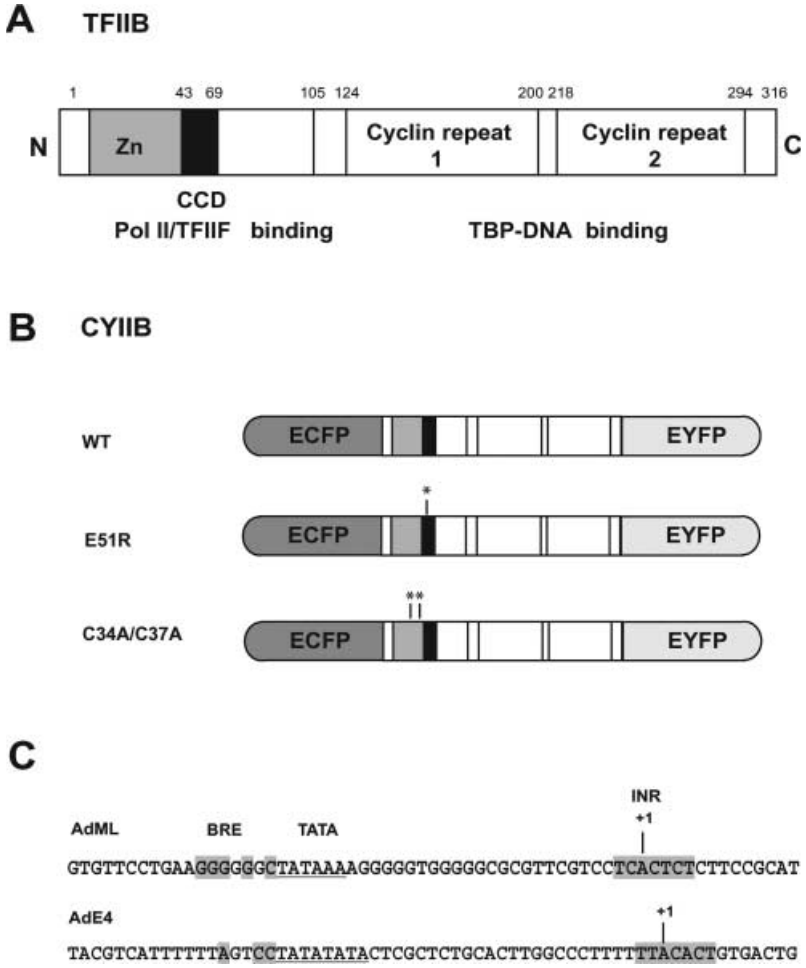

Fig. 1. Schematic depiction of (A) full-length human TFIIB (B) wild-type and mutant CYIIB, and (C) the nucleotide sequences of AdML and AdE4 promoter elements. Zn, zinc-ribbon domain; CCD, charged cluster domain; WT, wild-type; ECFP, enhanced cyan fluorescent protein; EYFP, enhanced yellow fluorescent protein; BRE, TFIIB recognition element; TATA, TATA box; INR, initiator sequence.

resonance energy transfer (FRET) [11–13]. We have generated various TFIIB constructs fused to enhanced cyan and yellow fluorescent protein (ECFP and EYFP) [14], which enable us to probe, in a time-dependent manner, the conformational change of TFIIB upon complexation with TBP bound with the AdML or AdE4 promoters [9]. The results indicate that the rate of TFIIB conformational change coupled with the TBP-promoter binding is significantly increased by GAL4–VP16 and depends on the sequence of the promoter.

Experimental procedures

Construction, overexpression, and purification of CYIIB and its derivatives

The gene encoding full-length human TFIIB [15] was amplified by PCR and inserted into pRSETb-YC2.1 [11] via *Sac*I and *Sph*I sites. This construct generated a fusion protein with ECFP preceding the N-terminus of TFIIB and EYFP following the C-terminus (CYIIB). ECFP-TFIIB was made by inserting the *TFIIB* gene into pRSETb-YC2.1 via *Sph*I and *Eco*RI sites. PCR-mediated site-directed mutagenesis was performed on CYIIB to generate C34A/C37A and E51R mutants. All clones were sequenced to ensure only the intended mutations were present.

Recombinant CYIIB proteins were expressed in *E. coli* strain BL21(DE3) (Novagen). Cultures were grown at 37 °C in LB medium containing 100 $\mu g \cdot mL^{-1}$ ampicillin and induced with 0.5 mM isopropyl thio-β-D-galactoside at 15 °C, overnight. Cells were harvested by centrifugation at 7000 ***g*** for 30 min at 4 °C. Cell pellets were suspended in lysis buffer (20 mM Tris/HCl, pH 7.5; 25 mM NaCl; 10 mM 2-mercaptoethanol; 1 mM phenylmethanesulfonyl fluoride; 20% glycerol; 3 mM $MgCl_2$; 0.5% NP40; 10 $\mu g \cdot mL^{-1}$ DNase I), sonicated, and centrifuged at 27 000 ***g*** for 30 min to remove debris. The supernatant was incubated with nickel chelate agarose and washed first with 1 M KCl, 2 mM imidazole in buffer A (20 mM Tris/HCl, pH 7.5; 20% glycerol; 10 mM 2-mercaptoethanol; 1 mM phenylmethanesulfonyl fluoride) and then with 300 mM KCl, 10 mM imidazole in the same buffer. CYIIB was eluted with 150 mM KCl, 300 mM imidazole in buffer A. The eluant was then further purified on a Superdex 200

HR 10/30 FPLC column using 20 mM Hepes pH 7.5, 150 mM KCl, 5% (v/v) glycerol, 5 mM dithiothreitol, 1 mM phenylmethanesulfonyl fluoride. CYIIB was eluted in a single peak and the fraction with the highest fluorescence intensity at 526 nm was used for FRET experiments. Glycerol was added to the sample at a final concentration of 20%, and the CYIIB was aliquoted and stored at −70 °C.

Overexpression and purification of TBP and Gal4-VP16

pET11d-TBP(yeast TBP residues 1–240) [16] was transformed into BL21(DE3) pLysS *E. coli* and protein synthesis was induced with 0.25 mM isopropyl thio-β-D-galactoside for 3 h at 27 °C. TBP was purified by nickel chelate affinity chromatography as described for CYIIB and then dialysis against SP buffer [20 mM Tris/HCl, pH 7.5; 20% (v/v) glycerol; 180 mM KCl; 5 mM $CaCl_2$; 5 mM dithiothreitol] overnight. Then the His_6-tagged TBP was digested by trypsin at 200 $\mu g \cdot mg^{-1}$ recombinant protein for 6 min on a rocker at 4 °C, yielding a truncated construct containing the conserved TBP core domain (49–240). The reaction was stopped by aminoethyl-benzene sulfonyl fluoride HCl (AEBSF) and protein solution was loaded onto a pre-equilibrated SP-Sepharose column. After washing with SP equilibration buffer, the TBP sample was eluted with 800 mM KCl in SP buffer. By adding 20 mM Tris/HCl and 60% glycerol, the protein solution was adjusted to 20 mM Tris/HCl, pH 7.5; 40% glycerol; 400 mM KCl; 5 mM dithiothreitol and stored at −70 °C.

Gal4(1–93)-VP16(413–490) in pRJR vector [17] was transformed into *E. coli* strain BL21(DE3) and expressed and purified as described for CYIIB.

Purification of promoter DNA fragments

The promoter DNA templates AdML and AdE4 in pGEM vector [18] were transformed into *E. coli* strain DH5α, grown overnight at 37 °C, and extracted by using the QIAfilter plasmid Giga kit (Qiagen). The plasmid DNA was cut by *Bam*HI and *Eco*RI, phenol/chloroform extracted and precipitated. After washing with 70% ethanol, the DNA pellet was dissolved in buffer A (10 mM Tris/HCl, pH 7.5; 1 mM EDTA; 0.35 M NaCl) and loaded onto a HiTrap Q column. The DNA fragment eluted with a 0.35 M to 2.0 M NaCl gradient and was confirmed on a native polyacrylamide Tris/borate/EDTA gel. Peak fractions were pooled, and the buffer for the pooled sample was exchanged with 10 mM Tris/HCl pH 7.5 and this sample was concentrated and stored at −20 °C.

Gel mobility shift assay

An adenovirus Major Late promoter fragment (nucleotides −50 to +22) was radiolabeled with [^{32}P]dATP[αP] using a Klenow fragment and then gel-purified. Bandshifts were performed as described previously using purified recombinant TBP, TFIIB and CYIIB [19]. Complexes were resolved by native gel electrophoresis (5% acrylamide) and visualized by autoradiography. Anti-human TFIIB Ig was prepared as described previously [18].

Fluorescence spectroscopy

All fluorescence spectra were recorded on a Shimadzu spectrofluorometer RF5301 using a 10 mm path-length quartz cuvette at room temperature. The fluorescence emission was monitored between 450 and 600 nm with excitation at 437 nm. The excitation and emission slit widths were 5 nm. Unless otherwise indicated, all measurements were performed in 20 mM Hepes, pH 7.5; 150 mM KCl; 5% (v/v) glycerol; 5 mM dithiothreitol and 1 mM phenylmethanesulfonyl fluoride. The fluorescence emission ratio was determined by dividing the integration of fluorescence intensities between 520 and 535 nm by that between 470 and 485 nm. Note that the absorbance spectrum of CYIIB in a range of 430 to 550 nm is essentially identical to that of a 1 : 1 mixture of ECFP and EYFP, confirming that an excitation at 437 nm is adequate for ECFP to transmit FRET to EYFP within the CYIIB fusion system. Fusing TFIIB to the C-terminus of ECFP does not change the fluorescence spectrum of ECFP, so as with fusing TFIIB to the N-terminus of EYFP.

For the kinetics measurements, a premixture of equimolar TBP and AdML or AdE4 promoter were added to CYIIB solution with or without ≈100 nM Gal4–VP16. The concentrations of CYIIB and its mutants E51R and C34A/C37A were determined by using EYFP's extinction coefficient of 84 000 $cm^{-1} \cdot M^{-1}$ at 514 nm (http://www.clontech.com; Protocol #PT2040-1) as well as the fluorescence intensity at 526 nm when excited at 514 nm. The concentration of TBP was determined by Bradford assay (Bio-Rad). The concentration of DNA was determined by A_{260}. The final concentrations of all components were adjusted to approximately 60 nM. After rapid mixing for ≈20 s, the 3D fluorescence spectra recording was started immediately for 20 min at 1 min intervals. For each sample, three or four measurements were performed. The emission ratio was calculated as described above and plotted against time. To the pseudo-first order approximation, observed changes in the emission intensity ratio at 476 and 526 nm were fitted by using Microsoft's EXCEL SOLVER to perform least-squares curve fitting, with $\Sigma(\delta^2)$ of 0.001. The observed rate constant k_{obs} was calculated from each set of data by nonlinear regression analysis using the following formula:

$$R_t = R_\infty + (R_0 - R_\infty) \times e^{-k_{obs}} \times t$$

where, R_0 is the initial emission ratio before adding TBP and promoters, R_t and R_∞ are the observed emission ratio at time t and at infinity, respectively. An error bar indicates the SD of each data point from the average value.

Results

Design and biochemical integrity of CYIIB

To gain more insight into the conformational variability of TFIIB, we employed GFP-based FRET methods [12,13]. A single polypeptide FRET-based indicator for TFIIB conformational change (hereafter referred to as CYIIB) was constructed by fusing ECFP (donor) and EYFP (acceptor) to the N- and C-terminus of TFIIB, via RMH and GGS peptide linker sequences, respectively (Fig. 1B). For all CYIIB constructs described in this study, we used a

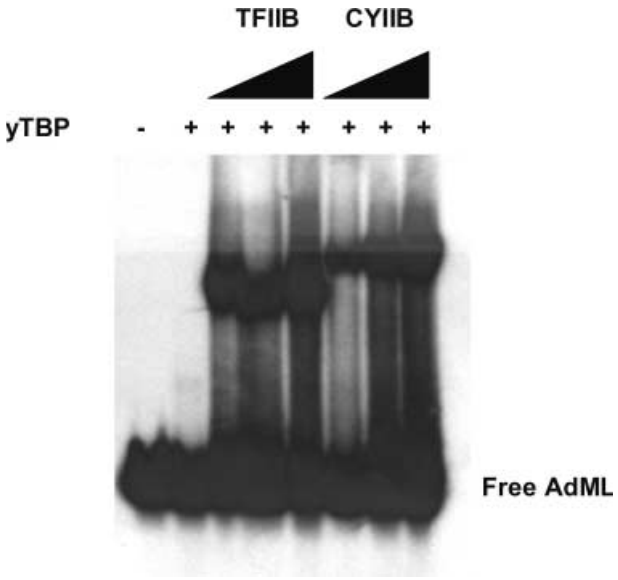

Fig. 2. Gel mobility shift assay showing that CYIIB forms a TBP-CYIIB-promoter complex. Recombinant TBP (2 ng) was added where indicated. Increasing amounts of TFIIB and CYIIB (5, 10, 20 ng) were added.

truncated version of ECFP that lacks G229-K239 at the C-terminus.

We first used gel mobility shift assays to assess the ability of CYIIB to bind to the TBP–DNA complex. Recombinant TBP and increasing amounts of either recombinant native TFIIB or CYIIB were incubated with a radio labeled AdML promoter fragment and the complexes were resolved by native gel electrophoresis (Fig. 2). TBP alone did not show a 'super shift' on the gel (known phenomenon when full-length TBP is used) and required the addition of either TFIIB or CYIIB. We also tested the ability of anti-TFIIB Ig to disrupt the ternary complex formation with CYIIB and indeed the antibody drastically abrogated the CYIIB–TBP–AdML complex formation. These results demonstrate that CYIIB is competent in forming a complex with TBP at the promoter. As expected from the fusion of the fluorescent tags, the CYIIB–TBP–DNA complex migrated at a slower rate than that observed of the TFIIB–TBP–DNA complex. Thus, the CYIIB fusion protein forms a defined complex with TBP at the AdML promoter.

We then investigated the spectroscopic properties of CYIIB. By exciting at 437 nm, the emission spectrum of wild-type CYIIB showed a double peak appearance typical for ECFP/EYFP-based FRET, one peak at 476 nm corresponding to ECFP and a more intense peak at 526 nm, arising mainly from EYFP (Fig. 3A). This energy transfer to the longer wavelength occurred only when ECFP and EYFP were fused to TFIIB. The observed emission ratio between 526 nm and 476 nm was 1.14 ± 0.01 for wild-type CYIIB. When the same experiment was performed on two separate constructs, ECFP–TFIIB and EYFP mixed at 1 : 1 ratio, we completely abolished the peak at 526 nm (Fig. 3B) and no FRET was observed. This was also true for a 1 : 1 mixture of ECFP and EYFP (Fig. 3C). These results demonstrate that the observed FRET is specific to CYIIB and therefore owing to the nature of TFIIB conformational state within the fusion system of CYIIB.

To further confirm whether the relatively high intensity of the 526 nm peak is due to FRET, we performed limited trypsin proteolysis on CYIIB. Within ≈10 min after addition of trypsin, a drastic reduction of the 526 nm peak was observed in parallel with an increase in intensity of the 476 nm peak (Fig. 3A). As ECFP and EYFP are both highly resistant to trypsin digestion [11], the protease must have cleaved TFIIB thus disenabling the NTD/CTD interaction. These results assured us that the enhanced fluorescence intensity at 526 nm in CYIIB was due to the intramolecular FRET between ECFP and EYFP fused at the two termini of CYIIB.

As GFP and its variants are known to be sensitive to pH and salt concentrations [14,20], we first examined the fluorescence characteristics of CYIIB against KCl and pH concentrations (Fig. 4A,B). When the concentration of KCl

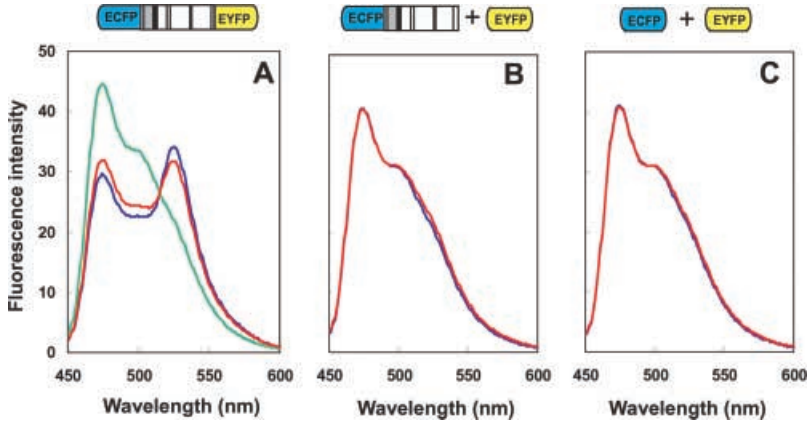

Fig. 3. Emission spectra of (A) wild-type CYIIB (B) a 1 : 1 mixture of ECFP-TFIIB and EYFP, and (C) a 1 : 1 mixture of ECFP and EYFP. Emission spectra of each sample (excitation at 437 nm) are shown in blue, those after the addition of TBP–AdML in red. An emission spectrum of trypsin-treated CYIIB is shown in green in panel A. The concentrations of CYIIB, ECFP–TFIIB, ECFP, EYFP, and AdML were all kept at approximately 60 nM.

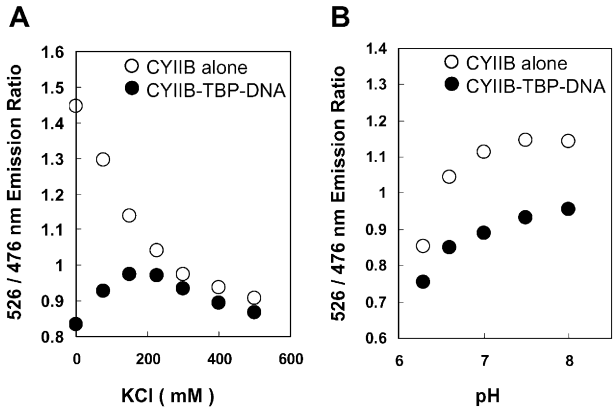

Fig. 4. Salt and pH effects on the FRET of CYIIB. (A) KCl concentration dependence of the emission ratio (526/476 nm) of CYIIB. (B) pH-dependence of the emission ratio (526/476 nm) of CYIIB. Data are obtained for wild-type CYIIB alone (open circle) and for the CYIIB–TBP–AdE4 complex (filled circle). For KCl titration experiments, 20 mM Hepes (pH 7.5) containing 5% glycerol and 5 mM dithiothreitol was used. For pH titration experiments, 20 mM Hepes was used for the range of 6.6–8.0 and 20 mM Mes for pH 6.3 (both buffers contained 150 mM KCl, 5 mM dithiothreitol, and 5% glycerol). Approximately 60 nM CYIIB was used.

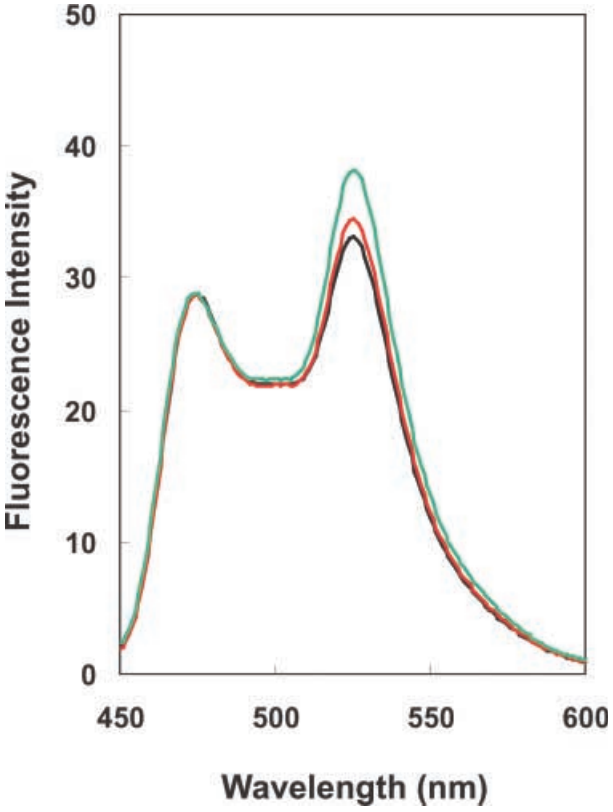

Fig. 5. Emission spectra of the wild-type CYIIB (black), E51R (red), and C34A/C37A (green). The spectra of the mutants are normalized to the spectrum of wild-type CYIIB using the peak maximum at 476 nm.

was increased from 0 to 500 mM, the emission ratio of apoCYIIB dropped drastically from 1.45 to 0.90. This is probably attributed to a weakened electrostatic interaction between the NTD and CTD at a high ionic strength, which promotes accumulation of the open conformation. Interestingly, the effect of ionic strength was abolished by the complex formation with AdE4-bound TBP, consistent with the extensive interaction of TFIIB with the promoter-bound TBP [21]. In both TBP-promoter bound or unbound states, the emission ratio was relatively constant between pH 6.6 and 8.0, while it started to drop below pH 6.6. This large decrease in the emission ratio at low pH is due to the pH sensitivity reported previously for EYFP [22]. Nevertheless, all measurements described below were performed in a 20 mM Hepes buffer (pH 7.5) containing 150 mM KCl, in which the pH and KCl concentration were kept constant throughout the entire experiments.

CYIIB mutants

In addition to wild-type CYIIB, we generated two CYIIB mutant constructs: E51R and C34A/C37A (Fig. 1B), the former representing a CCD mutant and the latter a Zn^{2+} ribbon mutant. The single mutant E51R in human TFIIB (equivalent to E62R in yeast TFIIB [23]) caused a downstream shift in the transcription start site at the AdE4 promoter, but not the AdML promoter [9]. Zn^{2+} binding site mutant, similar to the double point mutant C34A/C37A used in this study, has been shown to prevent recruitment of Pol II to the PIC [24] or not to support transcription *in vitro* [25].

Excitation of these two CYIIB mutants at 437 nm also produced a two peak appearance with a maximum at 476 and 526 nm (Fig. 5). When comparing the 526/476 nm emission ratio of E51R and C34A/C37A mutants to that of wild-type CYIIB, we found noticeable differences among those three constructs: the two mutants E51R and C34A/C37A displayed higher ratio (1.19 ± 0.01 and 1.32 ± 0.01, respectively) than wild-type CYIIB (1.14 ± 0.01).

TBP-promoter induced conformational change in CYIIB

We then examined the effect of TBP–AdML binding on the FRET efficiency observed for CYIIB (Fig. 3A). The ratio of the intensity between the peak of 526 nm and of 476 nm changed from 1.14 (apo-CYIIB) to 0.95 (complexed CYIIB). This change was not observed when CYIIB was mixed with TBP alone or with DNA alone. Furthermore, when TBP–AdML was added to a 1 : 1 mixture of ECFP–TFIIB and EYFP (Fig. 3B), no ratio change was observed. A 1 : 1 mixture of ECFP and EYFP (Fig. 3C) also showed no change. Finally, our gel filtration experiments indicated that CYIIB was predominantly monomeric below 10 μM, consistent with the reported dissociation constant of GFP monomer-dimer equilibrium (i.e. ≈100 μM) [26]. These results strongly support the decrease in EYFP fluorescence and increase in ECFP emission seen in CYIIB as a result of conformational change of TFIIB upon binding with TBP–AdML. A similar degree of TBP-promoter dependent change in emission ratio was also observed for CYIIB mutants; from 1.19 to 1.03 for E51R and 1.32 to 1.04 for C34A/C37A (Fig. 6A).

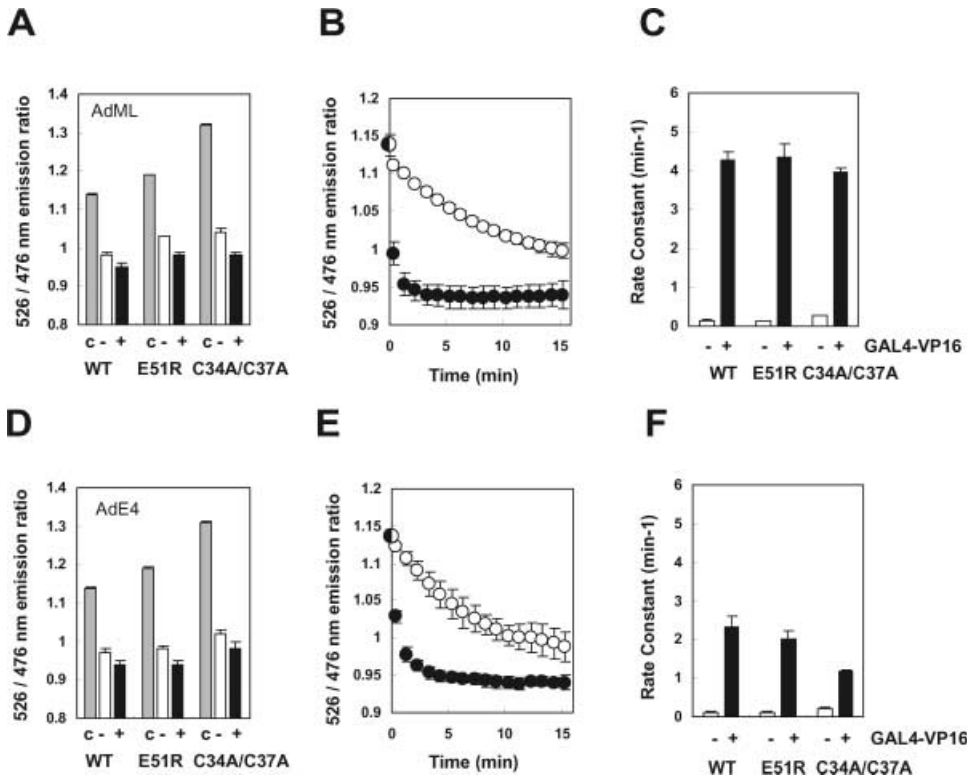

Fig. 6. Effects of TFIIB mutations on FRET for CYIIB and kinetic characterization of CYIIB. (A, D) Comparison of fluorescence emission ratios among wild-type CYIIB, E51R, and C34A/C37A. (B, E) Time-dependence of emission ratios upon addition of TBP-promoter in the absence (open circle) and in the presence of GAL4-VP16 (filled circle). (C, F) Comparison of the rate constants obtained for wild-type CYIIB, E51R, and C34A/C37A, using kinetic curves as shown in panel B and E. AdML and AdE4 (≈ 60 nM) were used as promoters for panel A–C and for panel D–F, respectively. In panels A, C, D, and F, – and + represent in the absence and in the presence of GAL4–VP16 (100 nM), and c is the control, representing CYIIB alone. Protein concentrations of CYIIB and the two mutants were all kept at ≈ 60 nM.

GAL4-VP16 accelerates the formation of a TFIIB–TBP–DNA complex

To gain insight into the kinetics of the TFIIB–TBP–promoter complex formation, we investigated the time course of FRET intensity after adding the TBP-promoter complex. When premixed TBP–AdML was added into the CYIIB solution we observed an immediate drop in the FRET ratio (the experimental dead-time is ≈ 20 s) (Fig. 6B). The k_{obs} was estimated to be 0.15 min with AdML promoter.

The presence of GAL4-VP16 in the initial solution of CYIIB altered drastically the time-dependence profile of the 526/476 nm emission ratio change upon the addition of premixed TBP-AdML (Fig. 6B). A much sharper drop of the emission ratio was observed (k_{obs} of 4.26 min), ≈ 27× larger relative to that seen without GAL4–VP16. These results are in excellent agreement with the previously reported value obtained by the gel-shift mobility assay of native TFIIB [27], indicating that the functional influence of fused ECFP/EYFP to TFIIB is relatively subtle or negligible as far as the complexation with the promoter-bound TBP is concerned.

Do the CYIIB mutations described above affect the rate constant for the CYIIB–TBP–promoter assembly? In the absence of GAL4–VP16, the k_{obs} obtained for E51R (0.14 ± 0.01 min^{-1}) was essentially identical to the value of wild-type CYIIB (Fig. 6C). When GAL4–VP16 was added to the initial solution of CYIIB the rate constant drastically increased almost 30× to 4.34 ± 0.36 min^{-1}, in a manner similar as that for wild-type CYIIB. In contrast, C34A/C37A produced a different pattern: without GAL4–VP16, C34A/C37A showed a higher k_{obs} (0.28 ± 0.01 min^{-1}), almost two times the value for wild-type CYIIB; while in the presence of GAL4–VP16 the k_{obs} increased only 14×, roughly half of the enhancement observed for wild-type CYIIB and E51R.

Promoter dependence of GAL4–VP16 activated TFIIB–TBP–promoter complex formation

Fairley *et al.* [9] recently reported that the sequence of the core promoter is critical for the selection of the transcription start site. This observation leads to the speculation that TFIIB can adopt different conformations depending on which core promoter it binds to. Furthermore, the TFIIB E51R mutant promotes aberrant transcription start site assembles at the core promoter, presumably due to its conformation differing from the wild-type TFIIB [9].

In order to investigate conformational and kinetic effects of different promoter sequences on TFIIB–TBP–promoter complex formation, we compared the two different promoter elements, AdML and AdE4 (Fig. 6). The observed rate constants for wild-type CYIIB and mutants E51R and C34A/C37A on TBP–AdML and TBP–AdE4 are summarized in Fig. 6C,F. Similar to what was seen for AdML, GAL4–VP16 increased the k_{obs} for all three constructs on AdE4 by a factor of 20 for both wild-type CYIIB and E51R (2.32 vs. 0.12 min^{-1} for wild-type and 2.01 vs. 0.11 min^{-1} for E51R) and by a factor of 5.6 for C34A/C37A (1.17 vs. 0.21 min^{-1}). Interestingly, the GAL4–VP16-dependent enhancement on the rate constant for AdE4 promoter was significantly smaller (approximately half) as compared to that observed for AdML promoter.

Discussion

It has been thought that a rearrangement of CTD and NTD orientation is crucial for the activation of TFIIB [4]. The lack of high-resolution structural data for full-length TFIIB, however, makes it unclear to what degree the conformation of TFIIB changes upon binding of the TBP-promoter complex. A recent study using small-angle X-ray scattering [28] suggests that NTD does make an intramolecular interaction with the CTD in apo TFIIB, yet how this changes upon binding to an TBP–DNA complex remained largely undefined. FRET is an extremely sensitive method for detecting a change in the proximity between donor and acceptor chromophores, ECFP and EYFP in our case, which are fused to the two termini of a target protein. With this structural constraint, it is fairly safe to assume that a change in FRET with CYIIB monitors a conformational change in TFIIB. Similar FRET-based conformational indicators have been successfully used for various cellular proteins such as calmodulin [11,29], caspases [30,31], and Ras/Rap1 [32].

The 526/476 nm emission ratio of CYIIB decreases upon binding to TBP complexed with two different promoters (1.14–0.95 for AdML and 1.14–0.98 for AdE4). As the conformational change of TFIIB probably involves a hinge motion of the domain linker, both the relative angle and distance between the NTD and CTD will probably be affected. Nevertheless, the decrease in the emission intensity ratio, observed for both AdML and AdE4, strongly suggests that TFIIB undergoes a change from a somewhat 'closed' conformational state in the apo form to a rather 'open' conformational state of the ternary complex form with promoter-bound TBP. By using the Förster equation [33], the observed decrease in emission intensity ratio could mean an increase in the ECFP-EYFP distance (from 55 Å to 58 Å), assuming that the Förster distance of ECFP and EYFP is 49 Å [34]. This small distance change between the two termini of TFIIB may suggest that the N-terminal Zn^{2+} ribbon domain still interacts with CTD, yet it can interact with other initiation factor(s) such as Pol II subunit(s) in order to properly position the initiation complex at the start site [4]. Alternatively, the observed FRET change represents a time-averaged value, and thus does not exclude a possibility that TFIIB exists as an extended conformation with certain lifetime. Nevertheless, such a dynamic conformational change is probably promoted by the CCD containing linker region (residues 43–105) which connects NTD and CTD in TFIIB. Indeed, the CCD mutation (E51R) affects the conformation of TFIIB, as evidenced by a higher FRET ratio observed with apo CYIIB.

Transcription is a time-dependent process which involves multiple steps in the molecular assembly of general transcription factors and Pol II [1,2]. A full understanding of this complex process depends on our ability to visualize and quantify individual molecular events with high spatial and temporal resolution in the cellular context. Our TFIIB-based FRET probes enabled us to characterize the time-dependent process of the formation of a TFIIB–TBP–TATA complex. One of the specific goals of this study is to assess how a transcriptional activator influences the rate of the TFIIB–TBP–TATA complex formation by employing FRET-based kinetic measurements, instead of conventional steady-state methods using gel electrophoresis assays. Our FRET data clearly indicate that VP16 indeed accelerates the TFIIB conformational change. In the presence of GAL4–VP16, the observed rate constant obtained for CYIIB with TBP bound to the AdML promoter (4.26 ± 0.23 min^{-1}) is significantly higher (> 20×) than that in the absence of GAL4–VP16 (0.15 ± 0.01 min^{-1}), indicating that this transcriptional activator enhances mainly the speed of the complex formation. On the other hand, when different promoters are used to investigate the CYIIB–TBP–promoter complex formation in the presence of GAL4-VP16, different rate constants were obtained: 4.26 min^{-1} for AdML and 2.32 min^{-1} for AdE4, indicating that the acceleration of the complex formation is dependent on the promoter. This relatively large difference in k_{obs} is somewhat diminished when GAL4–VP16 is absent (basal transcription case), yet the kinetics obtained for AdML promoter (0.15 min^{-1}) remains to be faster than that for AdE4 (0.12 min^{-1}). Thus, GAL4–VP16 enhances the effect of different promoters on the rate of TFIIB–TBP–DNA complex formation. These differences in the kinetic aspect of complex formation may be accounted for by the previous notion that the BRE element enhances the affinity of TFIIB towards the promoter-bound TBP [9]. While the AdML and AdE4 promoters both contain the TATA box, only the former sequence contains the BRE element upstream of the TATA box (Fig. 1C).

An interesting finding with the CYIIB mutants is that the 526/476 nm emission ratio is sensitive to mutations introduced to the N-terminal Zn^{2+} ribbon and CCD regions of TFIIB. The mutant E51R displayed a 4.4% larger ratio enhancement relative to wild-type CYIIB, while the mutant C34A/C37A produces even larger enhancement (16% relative to the wild-type). The results on E51R may parallel the recent studies which suggested that this mutation within the CCD region caused an alternation of the spatial orientation between the N- and C-terminal domain of TFIIB [9]. Even greater FRET change observed for the mutant C34A/C37A may suggest similar, but perhaps more drastic, conformational effects as observed for E51R. Further structural studies are required to define exact conformational changes accompanied by those mutations.

Acknowledgements

We thank Atsushi Miyawaki and Roger Tsien for providing us with the expression vectors for ECFP and EYFP, and Danny Reinberg for providing us with human TFIIB cDNA. This work was supported by grants from the Canadian Institutes of Health Research (CIHR) and the Cancer Research Society Inc. K. P. H. is supported by a National Cancer Institute of Canada Fellowship, L. M. E. by a Wellcome Prize Studentship, S. G. E. R. by a Wellcome Trust Senior Fellowship, M. G. by a CIHR Fellowship, and M. I. is a CIHR Senior Investigator.

References

1. Roeder, R.G. (1996) The role of general initiation factors in transcription by RNA polymerase II. *Trends Biochem. Sci.* **21**, 327–335.
2. Orphanides, G., Lagrange, T. & Reinberg, D. (1996) The general transcription factors of RNA polymerase II. *Genes Dev.* **10**, 2657–2683.
3. Hampsey, M. (1998) Molecular genetics of the RNA polymerase II general transcriptional machinery. *Microbiol. Mol. Biol. Rev.* **62**, 465–503.
4. Roberts, S.G. & Green, M.R. (1994) Activator-induced conformational change in general transcription factor TFIIB. *Nature* **371**, 717–720.
5. Hawkes, N.A., Evans, R. & Roberts, S.G. (2000) The conformation of the transcription factor TFIIB modulates the response to transcriptional activators *in vivo*. *Curr. Biol.* **10**, 273–276.
6. Reese, J.C. (2003) Basal transcription factors. *Curr. Opin. Genet. Dev.* **13**, 114–118.
7. Bagby, S., Kim, S., Maldonado, E., Tong, K.I., Reinberg, D. & Ikura, M. (1995) Solution structure of the C-terminal core domain of human TFIIB: similarity to cyclin A and interaction with TATA-binding protein. *Cell* **82**, 857–867.
8. Wu, W.H. & Hampsey, M. (1999) An activation-specific role for transcription factor TFIIB *in vivo*. *Proc. Natl Acad. Sci. USA* **96**, 2764–2769.
9. Fairley, J.A., Evans, R., Hawkes, N.A. & Roberts, S.G. (2002) Core promoter-dependent TFIIB conformation and a role for TFIIB conformation in transcription start site selection. *Mol. Cell Biol.* **22**, 6697–6705.
10. Evans, R., Fairley, J.A. & Roberts, S.G. (2001) Activator-mediated disruption of sequence-specific DNA contacts by the general transcription factor TFIIB. *Genes Dev.* **15**, 2945–2949.
11. Miyawaki, A., Llopis, J., Heim, R., McCaffery, J.M., Adams, J.A., Ikura, M. & Tsien, R.Y. (1997) Fluorescent indicators for Ca2+ based on green fluorescent proteins and calmodulin. *Nature* **388**, 882–887.
12. Truong, K. & Ikura, M. (2001) The use of FRET imaging microscopy to detect protein–protein interactions and protein conformational changes in vivo. *Curr. Opin. Struct. Biol.* **11**, 573–578.
13. Zhang, J., Campbell, R.E., Ting, A.Y. & Tsien, R.Y. (2002) Creating new fluorescent probes for cell biology. *Nat. Rev. Mol. Cell Biol.* **3**, 906–918.
14. Tsien, R.Y. (1998) The green fluorescent protein. *Annu. Rev. Biochem.* **67**, 509–544.
15. Ha, I., Roberts, S., Maldonado, E., Sun, X., Kim, L.U., Green, M. & Reinberg, D. (1993) Multiple functional domains of human transcription factor IIB: distinct interactions with two general transcription factors and RNA polymerase II. *Genes Dev.* **7**, 1021–1032.
16. Liu, D., Ishima, R., Tong, K.I., Bagby, S., Kokubo, T., Muhandiram, D.R., Kay, L.E., Nakatani, Y. & Ikura, M. (1998) Solution structure of a TBP-TAF (II), 230 complex: protein mimicry of the minor groove surface of the TATA box unwound by TBP. *Cell* **94**, 573–583.
17. Reece, R.J., Rickles, R.J. & Ptashne, M. (1993) Overproduction and single-step purification of GAL4 fusion proteins from *Escherichia coli*. *Gene* **126**, 105–107.
18. Hawkes, N.A. & Roberts, S.G. (1999) The role of human TFIIB in transcription start site selection *in vitro* and *in vivo*. *J. Biol. Chem.* **274**, 14337–14343.
19. Maldonado, E., Ha, I., Cortes, P., Weis, L. & Reinberg, D. (1990) Factors involved in specific transcription by mammalian RNA polymerase II: role of transcription factors IIA, IID, and IIB during formation of a transcription-competent complex. *Mol. Cell Biol.* **10**, 6335–6347.
20. Miyawaki, A. & Tsien, R.Y. (2000) Monitoring protein conformations and interactions by fluorescence resonance energy transfer between mutants of green fluorescent protein. *Methods Enzymol.* **327**, 472–500.
21. Nikolov, D.B., Chen, H., Halay, E.D., Usheva, A.A., Hisatake, K., Lee, D.K., Roeder, R.G. & Burley, S.K. (1995) Crystal structure of a TFIIB-TBP-TATA-element ternary complex. *Nature* **377**, 119–128.
22. Miyawaki, A., Griesbeck, O., Heim, R. & Tsien, R.Y. (1999) Dynamic and quantitative Ca2+ measurements using improved cameleons. *Proc. Natl Acad. Sci. USA* **96**, 2135–2140.
23. Pinto, I., Wu, W.H., Na, J.G. & Hampsey, M. (1994) Characterization of sua7 mutations defines a domain of TFIIB involved in transcription start site selection in yeast. *J. Biol. Chem.* **269**, 30569–30573.
24. Buratowski, S. & Zhou, H. (1993) Functional domains of transcription factor TFIIB. *Proc. Natl Acad. Sci. USA* **90**, 5633–5637.
25. Bangur, C.S., Pardee, T.S. & Ponticelli, A.S. (1997) Mutational analysis of the D1/E1 core helices and the conserved N- terminal region of yeast transcription factor IIB (TFIIB): identification of an N-terminal mutant that stabilizes TATA-binding protein-TFIIB-DNA complexes. *Mol. Cell Biol.* **17**, 6784–6793.
26. Phillips, G.N. Jr (1997) Structure and dynamics of green fluorescent protein. *Curr. Opin. Struct. Biol.* **7**, 821–827.
27. Bangur, C.S., Faitar, S.L., Folster, J.P. & Ponticelli, A.S. (1999) An interaction between the N-terminal region and the core domain of yeast TFIIB promotes the formation of TATA-binding protein-TFIIB-DNA complexes. *J. Biol. Chem.* **274**, 23203–23209.
28. Grossmann, J.G., Sharff, A.J., O'Hare, P. & Luisi, B. (2001) Molecular shapes of transcription factors TFIIB and VP16 in solution: implications for recognition. *Biochemistry* **40**, 6267–6274.
29. Truong, K., Sawano, A., Mizuno, H., Hama, H., Tong, K.I., Mal, T.K., Miyawaki, A. & Ikura, M. (2001) FRET-based in vivo Ca2+ imaging by a new calmodulin-GFP fusion molecule. *Nat. Struct. Biol.* **8**, 1069–1073.
30. Harpur, A.G., Wouters, F.S. & Bastiaens, P.I. (2001) Imaging FRET between spectrally similar GFP molecules in single cells. *Nat. Biotechnol.* **19**, 167–169.
31. Takemoto, K., Nagai, T., Miyawaki, A. & Miura, M. (2003) Spatio-temporal activation of caspase revealed by indicator that is insensitive to environmental effects. *J. Cell Biol.* **160**, 235–243.
32. Mochizuki, N., Yamashita, S., Kurokawa, K., Ohba, Y., Nagai, T., Miyawaki, A. & Matsuda, M. (2001) Spatio-temporal images of growth-factor-induced activation of Ras and Rap1. *Nature* **411**, 1065–1068.
33. Stryer, L. (1978) Fluorescence energy transfer as a spectroscopic ruler. *Annu. Rev. Biochem.* **47**, 819–846.
34. Patterson, G.H., Piston, D.W. & Barisas, B.G. (2000) Forster distances between green fluorescent protein pairs. *Anal. Biochem.* **284**, 438–440.

Supplementary material

The following material is available from http://blackwellpublishing.com/products/journals/suppmat/EJB/EJB3983/EJB3983sm.htm

Fig. S1. Optical properties of CYIIB and comparison with those of ECFP and EYFP. (A) Absorbance spectra of CYIIB (2.5 μM) shown in blue and of a 1 : 1 mixture of ECFP and EYFP (2.5 μM each) in red. (B) Emission spectra of ECFP–TFIIB shown in blue and ECFP in red (excitation at 437 nm). (C) Emission spectra of CYIIB shown in blue and EYFP in red (excitation at 514 nm). In B and C, the protein concentrations of CYIIB, ECFP and EYFP were all kept at ≈ 60 nM.

Fig. S2. Gel mobility shift assay showing that TBP and TFIIB or CYIIB can form a stable complex at the AdML promoter. recombinant TBP (2 ng) and 5 ng of either TFIIB or CYIIB were added as shown above the autoradiogram. Anti-TFIIB Ig or preimmune serum were included in the binding reaction where indicated. The anti-TFIIB Ig was described previously [18].